

Type II superconducting parameters of Tl-doped PbTe determined from heat capacity and electronic transport measurements

Y. Matsushita,¹ P. A. Wiancki,¹ A. T. Sommer,² T. H. Geballe,³ and I. R. Fisher³

¹*Department of Materials Science and Engineering and Geballe Laboratory for Advanced Materials, Stanford University, Stanford, California 94305, USA*

²*Department of Physics, Stanford University, Stanford, California 94305, USA*

³*Department of Applied Physics and Geballe Laboratory for Advanced Materials, Stanford University, Stanford, California 94305, USA*

(Received 25 April 2006; revised manuscript received 28 July 2006; published 23 October 2006)

Tl-doped PbTe ($\text{Pb}_{1-x}\text{Tl}_x\text{Te}$) is an anomalous superconductor with a remarkably high maximum T_c value given its relatively low carrier concentration. Here, we present results of systematic measurements of superconducting parameters for this material, for Tl concentrations up to $x=1.4\%$. We find that it is a type II, weak-coupled BCS superconductor in the dirty limit and discuss implications for the applicability of the charge Kondo model recently proposed to account for superconductivity in this system.

DOI: 10.1103/PhysRevB.74.134512

PACS number(s): 74.70.Dd, 74.25.Bt

I. INTRODUCTION

Tl-doped PbTe ($\text{Pb}_{1-x}\text{Tl}_x\text{Te}$) is a degenerate semiconductor, with a small carrier concentration of $\sim 10^{20}$ holes/cm³ or less.¹⁻⁴ However, it is observed to superconduct^{1,2} for Tl concentrations x beyond a critical value $x_c \sim 0.3\%$,⁵ with a maximum T_c of ~ 1.5 K for the highest Tl concentrations [Fig. 1(a)], comparable to more metallic systems (for instance, Al). Furthermore, thallium is the only impurity known to cause superconductivity in PbTe, even though other impurities are able to dope to similar carrier concentrations and similar densities of states.⁶ For comparison, other supercon-

ducting semiconductors, including SnTe, InTe, and GeTe, can be doped to much higher carrier concentrations (approaching 10^{22} cm⁻³) by a number of different chemical substitutions but have only lower or comparable T_c values.⁷ Given the anomalously high maximum T_c value of Tl-doped PbTe, combined with the unusual concentration dependence, there has been considerable discussion as to the role that the Tl impurities play in the superconductivity of this material.⁸⁻¹²

PbTe has a rocksalt structure and has been treated with reasonable success using ionic models (i.e., $\text{Pb}^{2+}\text{Te}^{2-}$).¹³ Thallium impurities substitute on the Pb site, and calculations have shown that Tl^+ is more stable than Tl^{3+} in the PbTe lattice.¹³ This implies that Tl impurities will act as acceptors, and indeed Hall measurements confirm that for small doping levels the hole concentration increases by one hole for every Tl impurity.³ Carrier freeze-out is not observed to the lowest temperatures, indicating that the dopant atoms do not behave as hydrogenlike impurities due to the large static dielectric constant ($\epsilon_0 \sim 1000$) of the host PbTe.⁶ However, for concentrations beyond a characteristic value, the Hall number $p_H = 1/R_{H}e$ is observed to rise at a much slower rate with x and does not increase beyond $\sim 10^{20}$ cm⁻³ [observed elsewhere at 77 K in Refs. 2, 14, and 15 and shown here for single crystals at 1.8 K in Fig. 1(b)], suggesting that the additional impurities act in a self-compensating manner. Significantly, within the uncertainty of these measurements, this characteristic concentration is the same as $x_c \sim 0.3\%$, the critical concentration required for superconductivity. It is remarkable that as x is increased beyond x_c , T_c rises linearly over two orders of magnitude from 15 mK for $x \sim 0.3\%$ to 1.5 K for $x \sim 1.5\%$, while the hole concentration appears to be approaching saturation and varies by less than a factor of 2.

This behavior, combined with the absence of any detectable magnetic impurities in the diamagnetic susceptibility, has been interpreted as evidence that the Tl impurities are present in a mixed valence state composed of a mixture of both Tl^+ and Tl^{3+} valences for $x > x_c = 0.3\%$.²⁻⁴ We recently argued⁵ that anomalies in the normal state resistivity of Tl-

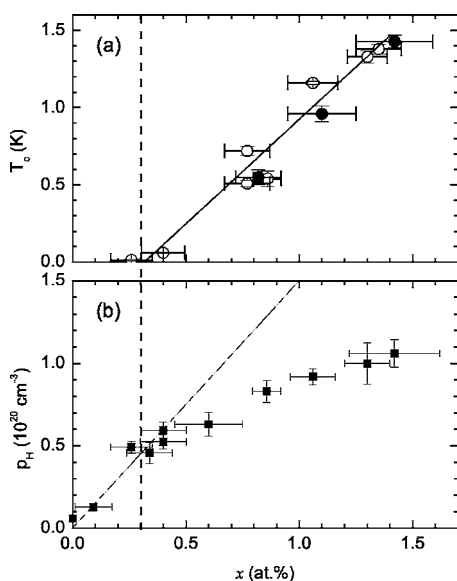


FIG. 1. (a) Superconducting transition temperatures T_c as a function of Tl concentration x . Closed symbols are obtained from heat capacity measurements, and open symbols are from resistivity data. The line is drawn to guide the eye. (b) Hall number $p_H = 1/R_{H}e$ as a function of Tl concentration x at 1.8 K. The solid line shows values calculated assuming one hole per Tl (Ref. 26). The vertical dashed line indicates critical Tl concentration x_c for superconductivity.

doped PbTe, that are present only for superconducting samples ($x > x_c$) and not for nonsuperconducting samples ($x < x_c$),¹⁶ might be associated with a charge Kondo effect involving these degenerate TI valence states. Within such a scenario, the quantum valence fluctuations associated with the TI impurities also provide a possible pairing mechanism for holes in the valence band of the host PbTe.¹²

In light of the anomalous behavior of TI-doped PbTe we have investigated the superconducting properties of single crystal samples for a range of TI concentrations up to the solubility limit of approximately 1.5%. In this paper, we present measurements of the heat capacity and H_{c2} and the resulting estimates for coherence length, penetration depth, Ginzburg-Landau parameter, and critical fields. Our measurements show that the material is a type II, weak-coupled BCS superconductor in the dirty limit. We discuss implications of these observations for the charge Kondo model.

II. SAMPLE PREPARATION AND EXPERIMENTAL METHODS

Single crystals of $\text{Pb}_{1-x}\text{TI}_x\text{Te}$ were grown by an unseeded physical vapor transport method. Polycrystalline source material was synthesized by combining PbTe, Te, and either TI_2Te or elemental TI in appropriate ratios and sintering at 600 °C, regrinding between successive sintering steps. For the crystal growth, broken pieces of source material were sealed in an evacuated quartz ampoule and placed in a horizontal tube furnace held at 750 °C for 7–10 days. A small temperature gradient of approximately 1 to 2 °C/cm allowed crystals to nucleate and grow at one or both of the cooler ends of the ampoule. Each vapor growth produced several well-formed crystals up to a few millimeters in size that could be cut and cleaved to prepare bars for thermodynamic and transport measurements. The thallium content was measured by electron microprobe analysis (EMPA) using PbTe, Te, and TI_2Te standards. Errors in TI content x shown in subsequent figures reflect the uncertainty of the microprobe method for such low dopant concentrations. The TI concentration for individual samples was observed to be homogeneous within the uncertainty of this measurement.

The heat capacity of single crystal samples was measured using a thermal relaxation technique in a Quantum Design Physical Property Measurement System. Crystals with a mass of approximately 10–15 mg were prepared with a flat surface for good thermal contact to the sample platform. Measurements were made in zero applied field and in a field $H=0.5\text{--}1\text{ T} > H_{c2}$. The field was oriented at an arbitrary angle to the crystal axes, depending on the orientation of the flat surface.

The upper critical field H_{c2} was measured for two representative values of the TI content x by following resistive transitions as a function of temperature for different applied magnetic fields. The resistivity was measured using geometric bars cleaved from the larger as-grown crystals, such that the current flowed along the [100] direction while the magnetic field was oriented parallel to the equivalent [001] direction. Electrical contact was made using Epotek H20E silver epoxy on sputtered or evaporated gold pads and showed

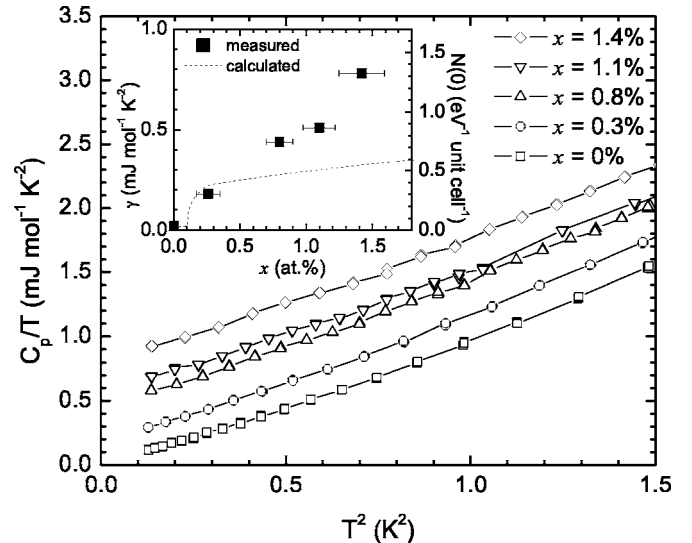


FIG. 2. Heat capacity of $\text{Pb}_{1-x}\text{TI}_x\text{Te}$ single crystals, shown as C_p/T vs T^2 , for representative TI concentrations. For superconducting samples, data were taken in an applied field $H=0.5\text{--}1\text{ T} > H_{c2}$. The inset shows electronic contribution γ (left axis) and density of states at the Fermi level $N(0)$ (right axis) as a function of TI concentration x . The dashed line shows values calculated from known PbTe band parameters and measured values of the Hall number, as described in the main text. The rapid increase in calculated values of γ at $\sim 0.1\%$ corresponds to the chemical potential entering the heavier Σ band (Ref. 26).

typical contact resistances of 1–4 Ω . Resistivity measurements were made at 16 Hz and with current densities in the range of 25 mA/cm² (corresponding to a current of 100 μA for low-temperature measurements) to 1 A/cm² at higher temperatures. To check for heating effects, resistivity data were taken for different current densities and for warming and cooling cycles for each sample. Hall effect data were also collected for several TI concentrations at 1.8 K. The Hall voltage was obtained from linear fits to the transverse voltage for fields between -9 and 9 T.

III. RESULTS

Heat capacity data for representative TI concentrations are shown in Fig. 2 as C_p/T vs T^2 for applied fields that totally suppress the superconductivity. For all samples there is a slight curvature in the data even at low temperatures. This curvature was observed previously for undoped PbTe samples and was attributed to possible softening of TO phonon modes.¹⁷ Data for TI-doped PbTe samples are essentially parallel to those for undoped samples indicating that the phonon contribution is not affected by TI substitution and that reasonable comparisons of the electronic contribution can be made between different dopings.¹⁸ Data were fit to $C/T = \gamma + \beta T^2 + \delta T^4$ from the base temperature (0.3 K) up to 1 K. From $\beta = N(12\pi^4/5)R\Theta^{-3}$, where $R=8.314\text{ J}/(\text{mol K})$ and $N=2$ for PbTe, we estimate $\Theta_D=168\pm 4\text{ K}$ for $x=0\%$, which is consistent with previous reports.^{17,19} Thallium substitution does not substantially affect this value but causes a clear increase in the electronic contribution γ , suggesting a rapid

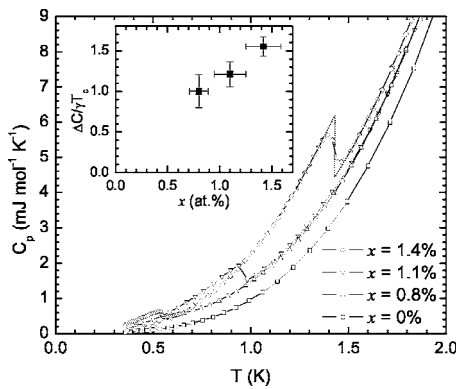


FIG. 3. C_p vs T in zero applied field showing the superconducting anomaly for several TI concentrations x . Dashed lines show the geometric construction used to obtain ΔC and T_c for $x=1.4\%$. Inset shows $\Delta C/\gamma T_c$ as a function of x . Uncertainty in $\Delta C/\gamma T_c$ is derived principally from errors in the geometric construction used to estimate ΔC .

rise in the density of states with x . Values of γ obtained from the above fits are shown in the inset to Fig. 2 as a function of TI concentration x and are in broad agreement with previously published values for polycrystalline samples.²⁰

Heat capacity data in zero field are shown in Fig. 3 for representative TI concentrations with T_c above 0.3 K. T_c values were obtained from the midpoint of the heat capacity anomaly and agree well with data obtained from resistive transitions [Fig. 1(a)]. The jump at T_c , ΔC , can be estimated using a standard geometric construction extrapolating normal state and superconducting state behaviors towards T_c , as indicated by dashed lines for $x=1.4\%$ in Fig. 3. Resulting estimates of $\Delta C/\gamma T_c$ are shown in the inset to Fig. 3 as a function of TI concentration x . The value for the highest TI concentration, $x=1.4\%$, is $\Delta C/\gamma T_c=1.55\pm 0.12$, which is close to the weak coupling BCS result of 1.43. As x is reduced, the data show a small but significant systematic variation, tending towards a smaller value for smaller TI concentrations. The smallest value, 1.00 ± 0.20 , is recorded for $x=0.8\%$, which is the lowest TI concentration for which we can confidently extract ΔC given the base temperature of our instrument.

The upper critical field $H_{c2}(T)$ was determined from resistivity measurements for two representative TI concentrations. Representative data, showing the uniform suppression of the superconducting transition in an applied field, are shown in Fig. 4 for $x=1.4\%$. An estimate of T_c was obtained from the midpoint of the resistive transition for each applied field. Resulting H_{c2} curves are shown in Fig. 5 for $x=1.1\%$ and 1.4% . Error bars indicate the width of the superconducting transition measured by the difference in temperature between 10% and 90% of the resistive transition. The upper critical field at zero temperature $H_{c2}(T=0)$ can be estimated from these data using the Werthamer-Helfand-Hohenberg approximation²¹

$$H_{c2}(0) = 0.69(dH_{c2}/dT)_T T_c. \quad (1)$$

Resulting values for $x=1.1\%$ and 1.4% are approximately 3900 and 6000 Oe, respectively (Table I) and are consistent

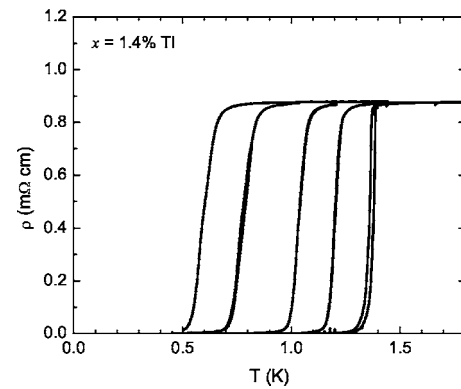


FIG. 4. Representative resistivity data for $x=1.4\%$, showing the superconducting transition as a function of temperature for different magnetic fields (0, 108, 1083, 2166, 3791, and 4875 Oe) applied parallel to the [001] direction.

with reasonable extrapolations of the lowest temperature data in Fig. 5 and previous reports.² The errors in $H_{c2}(0)$ listed in Table I are estimated from the difference between the above approximation and a parabolic fit to the observed data.

Superconducting parameters such as the coherence length and penetration depth are dependent on the electron mean free path $l=v_F\tau=v_F\mu m^*/e$, where v_F is the Fermi velocity and μ is the hole mobility. From Hall effect measurements at 1.8 K, we find that the Hall number p_H is $\sim 9 \times 10^{19} \text{ cm}^{-3}$ for $x=1.1\%$ and $\sim 1 \times 10^{20}$ for $x=1.4\%$ [Fig. 1(b)]. Taking into account the existence of both light and heavy holes at the L and Σ points in the Brillouin zone, respectively,²⁶ we assume the elastic scattering limit holds at low temperatures such that $l_L=l_\Sigma=l$. The Fermi level then lies in the range 190–210 meV below the top of the valence band. Consequently, average values of v_F are $\sim 1.4 \times 10^6$ m/s for the L holes and $\sim 1 \times 10^5$ m/s for the Σ holes. Combining these data with measured values of the residual resistivity,⁵ we find the hole mobility μ is approximately $100 \text{ cm}^2 \text{ V}^{-1} \text{ s}^{-1}$ for $x=1.1\%$ and $60 \text{ cm}^2 \text{ V}^{-1} \text{ s}^{-1}$ for $x=1.4\%$ (these values being similar for both L and Σ bands). The resulting values for l are listed in Table I. The principle contribution to the uncertainty in this quantity arises from errors in the geometric

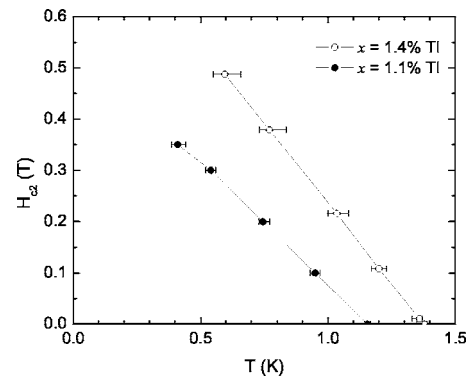


FIG. 5. Temperature dependence of H_{c2} for $x=1.1\%$ and 1.4% with the field parallel to the [001] direction. Error bars were determined as described in the main text. Lines are drawn to guide the eye.

TABLE I. Superconducting parameters of $\text{Pb}_{1-x}\text{Tl}_x\text{Te}$ for two representative Tl concentrations.

	$x=1.1\pm 0.1$ at. %	$x=1.4\pm 0.1$ at. %
T_c	1.16 ± 0.01 K	1.38 ± 0.03 K
$H_{c2}(0)$	0.39 ± 0.04 T	0.60 ± 0.07 T
l	32 ± 8 Å	19 ± 5 Å
$\xi(0)$	290 ± 15 Å	240 ± 14 Å
ξ_0	2600 ± 700 Å	3000 ± 850 Å
v_F	$2.2\pm 0.6\times 10^5$ m/s	$3.0\pm 0.8\times 10^5$ m/s
λ_L	1600 ± 80 Å	1500 ± 120 Å
λ_{eff}	1.4 ± 0.4 μm	1.9 ± 0.5 μm
κ	48 ± 12	79 ± 20
H_c	57 ± 14 Oe	54 ± 13 Oe
H_{c1}	3 ± 0.8 Oe	2 ± 0.5 Oe

factor used to calculate the resistivity of these samples. Propagation of this error is the dominant effect in the uncertainties of subsequent derived quantities, including ξ_0 and λ_{eff} .

The Ginzburg-Landau coherence length $\xi(0)$ is calculated from $H_{c2}(0)$ by

$$H_{c2}(0) = \frac{\Phi_0}{2\pi\xi^2(0)}, \quad (2)$$

where $\Phi_0 = 2.0678 \times 10^{-15}$ T m². Estimates for $\xi(0)$ are 290 Å for $x=1.1\%$ and 240 Å for $x=1.4\%$ (Table I) and should be independent of orientation for this cubic material. The small values of l imply that the material is in the dirty limit with $l < \xi_0$. Therefore the intrinsic coherence length ξ_0 can be extracted from the approximation $\xi(0) \sim (l\xi_0)^{1/2}$, where the values are listed in Table I. In comparison, the BCS expression for ξ_0 is

$$\xi_0 = \frac{\alpha\hbar v_F}{k_B T_c}, \quad (3)$$

where the BCS value of α is 0.18. Using values of ξ_0 derived from the dirty limit approximation, we find v_F estimated from this formula (given in Table I) is between those calculated separately for the L and Σ holes. This is consistent with a mixed contribution from both carrier types due to the substantial scattering implied from the short mean free path.

The London penetration depth for two carrier types is given by

$$\frac{1}{\lambda_L^2} = \frac{\mu_0 n_L e^2}{m_L} + \frac{\mu_0 n_\Sigma e^2}{m_\Sigma}, \quad (4)$$

where the superfluid densities n_L and n_Σ are approximated as the carrier densities for each carrier type, and m_L and m_Σ are the effective masses of each band. The corresponding values of λ_L are listed in Table I and are almost independent of orientation. In the dirty limit, we can estimate the effective penetration depth from

$$\lambda_{\text{eff}} = \lambda_L (\xi_0/l)^{1/2}, \quad (5)$$

values of which are given in Table I. These estimates are in good agreement with microwave conductivity measurements that show $\lambda(0) \sim 2$ to 3 μm for $x=1.4\%$.²² Finally, we find the Ginzburg-Landau parameter using $\kappa = \lambda_{\text{eff}}/\xi(0)$ and estimate the thermodynamic critical field H_c and the lower critical field H_{c1} from the relationships $H_{c2} = \sqrt{2}\kappa H_c$ and $H_{c1} = \frac{H_c}{\sqrt{2}\kappa} \ln \kappa$ (Table I).

IV. DISCUSSION

The above results indicate that Tl-doped PbTe is a type II, BCS superconductor in the dirty limit, which is not too surprising given that the material is a doped semiconductor. To a large extent this observation rules out the possibility of more exotic scenarios for the superconductivity, such as condensation of preformed pairs, at least for the highest Tl concentrations. Here, we discuss some implications for the charge Kondo model that we have previously proposed for this material and consider alternative explanations. First, we briefly reiterate the salient features of the charge Kondo model relevant to understanding these data.

The idea of a charge Kondo effect associated with degenerate valence (charge) states of a valence-skipping element was first discussed by Taraphder and Coleman,²³ and was later reexamined in the limit of dilute impurities for the case $T_c \sim T_K$ by Dzero and Schmalian.¹² Weak hybridization of these degenerate impurity states with conduction electrons (or in the case of Tl-doped PbTe, with valence band holes) results in a Kondo-like effect with various parallels to the more common magnetic case. Here, the pseudospins correspond to zero or double occupancy of an impurity orbital, which can be described in terms of a negative effective U . The degeneracy of the two valence states in PbTe is not accidental but emerges naturally from the doping effect of the Tl impurities themselves.¹² For values of the chemical potential less than a characteristic value μ^* , the impurities are all present as one valence (Tl⁺), which act to dope the material. As more impurities are added, eventually a value of the chemical potential μ^* is reached for which the two valence states are degenerate, and at which value the chemical potential is then pinned.¹² The resulting charge Kondo effect, if present, clearly requires that hybridization between the impurity states and the host material be relatively weak. The semiconducting nature of the host PbTe would naturally provide an environment in which the local density of states at the impurity sites is rather small.

Now, we discuss the origin of the enhanced electronic contribution to the heat capacity seen in Fig. 2. The density of states at the Fermi energy, $N(0)$, can be estimated from the linear term γ in the heat capacity, and resulting values are shown on the right axis of the inset to Fig. 2. Part of the observed increase in $N(0)$ with x can be attributed to band filling effects, since the Hall number continues to rise slowly with x even for $x > x_c = 0.3\%$ [Fig. 1(b)]. However, as has been discussed elsewhere,²⁰ the observed heat capacity is substantially larger than expected from these band filling effects alone (dashed line in the inset to Fig. 2 calculated from

the measured Hall coefficient using published band parameters and assuming that the band offset does not change with TI doping), implying the presence of additional states associated with the TI impurities. Within the charge Kondo model, the additional contribution would arise from the Abrikosov-Suhl resonance that develops at E_F for temperatures below T_K . If this is the case, then in principle we can estimate the concentration of Kondo impurities using the crude approximation $\gamma T_K \sim R \ln 2$ per mole of impurities. For $x=1.4\%$, the observed γ is $0.46 \text{ mJ mol}^{-1} \text{ K}^{-2}$ larger than the expected band contribution based on the measured Hall coefficient (inset to Fig. 2). If this enhancement is due to Kondo physics, then for $T_K \sim 6 \text{ K}$ (the value estimated in Ref. 5 for $x=0.3\%$), the concentration of Kondo impurities is approximately $7 \times 10^{18} \text{ cm}^{-3}$. In comparison, $x=1.4\%$ corresponds to a TI concentration of $2 \times 10^{20} \text{ cm}^{-3}$. Hence if a charge Kondo description is appropriate for this material, and if the Kondo temperature is $\sim 6 \text{ K}$, then only a small fraction ($\sim 3\%$) of the TI impurities are contributing to this effect. Within the charge Kondo model outlined above, this would imply that the TI impurities in PbTe must be characterized by a range of μ^* values, such that only the subset of impurities for which $\mu = \mu^*$ have degenerate valence states.

There are other observations that appear to support this tentative conclusion. As we had previously noted,⁵ the magnitude of the resistivity anomaly is also less than what would be expected if all of the TI impurities were contributing to the Kondo effect. Data for lower TI concentrations, for which a reasonable fit of the low-temperature data can be made over an extended temperature range, indicated that approximately 1% of the TI impurities contribute to the Kondo behavior.⁵ This is in broad agreement with the value deduced above from the heat capacity enhancement. In addition, the Hall number is observed to continue to rise for $x > x_c$ [Fig. 1(b)], implying that the chemical potential is not pinned at one precise value, but rather is slowed in its progress as x increases, also consistent with a distribution of μ^* values.

Invoking Kondo physics of course implies a temperature dependence to the enhancement of γ for temperatures above T_K . Our measurements (Fig. 2) show that the enhancement to γ is temperature independent for temperatures between 0.3 and 1 K. However, uncertainty in this difference grows rapidly at higher temperatures due to the increasingly large phonon contribution to the heat capacity. As a result, we cannot unambiguously extract the temperature dependence of any heat capacity enhancement beyond the estimated Kondo temperature of 6 K.

Within a BCS scenario, T_c varies exponentially with $-1/N(0)V$, where V is the pairing interaction. Figure 6 shows $\ln(T_c)$ vs $1/\gamma$ for samples with $x > x_c$. For samples with $T_c > 0.5 \text{ K}$, both parameters were extracted from the same physical crystal. However, for samples with a lower critical temperature, T_c was determined from resistivity measurements on different crystals from the same growth batch, introducing additional errors due to uncertainty in the TI concentration. As can be seen, $\ln(T_c)$ scales approximately linearly with $1/\gamma$ within the uncertainty of the measurements. For a constant V , this would imply that the observed trend in T_c with x [Fig. 1(a)] is due to the increasing density of states (inset to Fig. 2). However, the situation is less clear

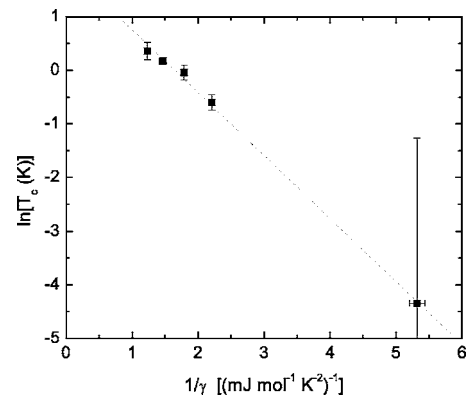


FIG. 6. Plot of $\ln(T_c)$ vs $1/\gamma$. The dashed line is a guide for the eye.

if the charge Kondo picture is applicable, in which case V depends strongly on the TI concentration,¹² and the enhancement in $N(0)$ derives from Kondo physics. In the case of a superconductor with magnetic impurities, although $N(0)$ is enhanced by this effect, the superconductivity is nevertheless suppressed for $T \sim T_K$ due to the pair-breaking effect associated with the rapid fluctuations in the magnetic moment.^{24,25} In the case of the charge Kondo model, the situation is slightly more complex because the impurities now provide both a local pairing mechanism as well as a pair-breaking effect close to T_K . Consequently, the range of temperatures over which it is anticipated that T_c will be suppressed is predicted to be much lower than T_K ,¹² in contrast to the case of magnetic impurities. Hence for the case $T_c \sim T_K$, the superconductivity can in principle benefit from the enhancement in $N(0)$ due to the charge Kondo effect in a way that it cannot for magnetic impurities. The observed trend shown in Fig. 6 may reflect this effect, but it is difficult to obtain quantitative estimates of the relative contributions to T_c from the enhancement in $N(0)$ and the pairing interaction itself in this crossover regime of $T_c \sim T_K$.¹²

In the charge Kondo model, if T_c is large compared to T_K , then the pseudospin moment is unscreened at T_c , in which case the superconductivity is born from preformed pairs. In this limit, one would anticipate a much smaller anomaly in the heat capacity $\Delta C/\gamma T_c$ than the BCS result of 1.43. As noted in Sec. III, this is clearly not the case for the highest TI concentrations, consistent with our previous observation that $T_c \sim T_K$ for this material.⁵ However, it is difficult to understand the observed x dependence of $\Delta C/\gamma T_c$ within this same picture. Since T_c decreases with decreasing x [Fig. 1(a)], one would expect the superconductivity to become more BCS-like at lower TI concentrations. Instead, we find that $\Delta C/\gamma T_c$ becomes substantially smaller as x is reduced (inset to Fig. 3). Experiments are in progress to measure the heat capacity of samples with yet smaller TI concentrations to even lower temperatures to see whether this trend continues.

Could the superconductivity in TI-doped PbTe have its origin in more mundane physics after all? While the data presented here enable us to characterize this material as a BCS superconductor, they do not allow us to distinguish between different pairing mechanisms. As we have previously argued,⁵ many aspects of the observed thermodynamic and

transport properties are suggestive of charge Kondo physics. Moreover, the uniqueness of the TI impurities, being the only dopant to cause superconductivity in this material, cannot be ignored. Nevertheless, in the absence of experiments directly probing the TI valence (which are currently in progress), we cannot rule out less exciting possibilities, including the formation of a narrow impurity band with a relatively large density of states. In such a case, the pairing interaction would most likely be phonon mediated, though the substantial residual resistance might argue that strong Coulomb scattering also plays a role. The observed low-temperature resistivity anomaly would then presumably have its origin in some form of weak localization, though the temperature and field dependence of this feature appear to argue against such a scenario.⁵

V. CONCLUSIONS

In summary, we have shown that TI-doped PbTe is a type II, BCS superconductor in the dirty limit. None of these observations is in disagreement with the charge Kondo model

previously described, though they do put some limitations on its applicability. Specifically, the relatively small enhancement of the electronic contribution to the heat capacity implies that if a charge Kondo description is appropriate then only a small fraction of the TI impurities can be participating in the Kondo physics. Within the model described in Ref. 12, this can be understood in terms of a distribution of μ^* values, such that only a subset of the TI impurities have both valence states exactly degenerate for a particular value of the chemical potential within this range, though this has yet to be experimentally verified.

ACKNOWLEDGMENTS

We gratefully thank J. Schmalian, M. Dzero, M. R. Beasley, and B. Mozyshes for numerous helpful discussions. We also acknowledge Robert E. Jones for technical assistance with EMPA measurements. This work was supported by the DOE, Office of Basic Energy Sciences, under Contract No. DE-AC02-76SF00515. I.R.F. was also supported by the Alfred P. Sloan and Terman Foundations.

-
- ¹I. A. Chernik and S. N. Lykov, *Sov. Phys. Solid State* **23**, 817 (1981).
²S. A. Némov and Y. I. Ravich, *Phys. Usp.* **41**, 735 (1998).
³V. I. Kaidanov and Y. I. Ravich, *Sov. Phys. Usp.* **28**, 31 (1985).
⁴B. A. Volkov, L. I. Ryabova, and D. R. Khokhlov, *Phys. Usp.* **45**, 819 (2002).
⁵Y. Matsushita, H. Bluhm, T. H. Geballe, and I. R. Fisher, *Phys. Rev. Lett.* **94**, 157002 (2005).
⁶R. Dornhaus, G. Nimtz, and B. Schlicht, *Narrow-Gap Semiconductors*, Vol. 98 of Springer Tracts in Modern Physics (Springer-Verlag, New York, 1983).
⁷J. K. Hulm, M. Ashkin, D. W. Deis, and C. K. Jones, *Prog. Low Temp. Phys.* **6**, 205 (1970).
⁸B. Y. Mozyshes and I. A. Drabkin, *Sov. Phys. Solid State* **25**, 1139 (1983).
⁹H. B. Schuttler, M. Jarrell, and D. J. Scalapino, *Phys. Rev. B* **39**, 6501 (1989).
¹⁰J. E. Hirsch and D. J. Scalapino, *Phys. Rev. B* **32**, 5639 (1985).
¹¹M. V. Krasin'kova and B. Y. Mozyshes, *Sov. Phys. Solid State* **33**, 202 (1991).
¹²M. Dzero and J. Schmalian, *Phys. Rev. Lett.* **94**, 157003 (2005).
¹³K. Weiser, *Phys. Rev. B* **23**, 2741 (1981).
¹⁴H. Murakami, W. Hattori, and R. Aoki, *Physica C* **269**, 83 (1996).
¹⁵K. G. Gartsman, T. B. Zhukova, and S. A. Némov, *Inorg. Mater.* **21**, 426 (1985).
¹⁶I. R. Fisher, Y. Matsushita, H. Bluhm, and T. H. Geballe, *Proc. SPIE* **5932**, 59321Y (2005).
¹⁷A. J. Bevelo, H. R. Shanks, and D. E. Eckels, *Phys. Rev. B* **13**, 3523 (1976).
¹⁸I. A. Chernik and S. N. Lykov, *Sov. Phys. Solid State* **23**, 1724 (1981).
¹⁹Y. I. Ravich, B. A. Efimova, and I. A. Smirnov, *Semiconducting Lead Chalcogenides* (Plenum Press, New York, 1970).
²⁰I. A. Chernik and S. N. Lykov, *Sov. Phys. Solid State* **23**, 2062 (1981).
²¹N. Werthamer, E. Helfand, and P. Hohenberg, *Phys. Rev.* **147**, 295 (1966).
²²R. J. Ormeno, P. J. Baker, and C. E. Gough (private communication).
²³A. Taraphder and P. Coleman, *Phys. Rev. Lett.* **66**, 2814 (1991).
²⁴M. B. Maple, W. A. Fertig, A. C. Mota, L. E. DeLong, D. Wohlleben, and R. Fitzgerald, *Solid State Commun.* **11**, 829 (1972).
²⁵E. Muller-Hartmann and J. Zittartz, *Phys. Rev. Lett.* **26**, 428 (1971).
²⁶The valence band maximum is centered at the L points of the Brillouin zone and consists of relatively light holes characterized by $m_l=0.31m_0$ and $m_t=0.022m_0$ [R. Dornhaus, G. Nimtz, and B. Schlicht, *Narrow-Gap Semiconductors*, Vol. 98 of Springer Tracts in Modern Physics (Springer-Verlag, New York, 1983)]. Small deviations from nonparabolicity can be safely ignored in estimating approximate values for the Fermi level. Somewhat less is known of the secondary band maximum centered at the Σ points in the Brillouin zone. Reasonable estimates were reported close to $m_\Sigma \sim m_0$ with an anisotropy of ~ 10 [B. F. Gruzinov, I. A. Drabkin, and Yu. I. Ravich, *Sov. Phys. Semicond.* **13**, 315 (1979)]. These holes are substantially more massive and therefore dominate the density of states. In estimating the Fermi energy and other electronic parameters from Hall effect measurements, we have used the appropriate two-band model including the given anisotropies and have assumed that the band offset (170 meV) does not vary with x . Since the mobilities of these two bands are very similar in the elastic limit, the actual hole concentration p does not differ significantly from $p_H=1/R_H e$.